Journal of Alloys and Compounds 509 (2011) 7317–7323

Contents lists available at ScienceDirect

Journal of Alloys and Compounds

journal homepage: www.elsevier.com/locate/jallcom

Multiple-barrier distribution behavior of Mo/p-GaTe fabricated with sputtering

Murat Gülnahar*, Hasan Efeoğlu

Atatürk University, Faculty of Engineering, Department of Electrical and Electronics Engineering, 25240 Erzurum, Turkey

ARTICLE INFO

Article history:
Received 12 July 2010
Received in revised form 28 March 2011
Accepted 30 March 2011
Available online 6 April 2011

Keywords:
Schottky barrier anomalies
Gaussian distribution
Richardson constant
Schottky diode
GaTe
Layered crystal

ABSTRACT

A Molybdenum Schottky diode on unintentionally doped p-GaTe was fabricated using DC sputtering. I–V characteristics of the fabricated diode were measured as a function of temperature at the range of 50–300 K. The barrier parameters of Mo/p-GaTe are interpreted using thermionic emission theory and inhomogeneities observed in the barrier are characterized with Gaussian distribution approach on the basis of parallel conduction model. The barrier height and the ideality factor values at 300 K and at 80 K of Mo/p-GaTe were calculated to be 0.581 eV, 1.097 and 0.472 eV, 1.349, respectively. The barrier parameters changed resolutely at 140–300 K temperature range and a strong temperature dependence was observed below 130 K. The weighting coefficients, standard deviations and mean barrier heights were calculated for sub distributions. Richardson plot was interpreted with a new approach and Richardson constant was found to be 117.96 AK^{-2} cm^{-2} for p-GaTe.

1. Introduction

The field of inhomegeneity of Schottky barrier constitutes one of the main research fields over metal semiconductor contact. So far, to interpret the anomalies arisen from the nature of the interface between metal and semiconductor, various approaches and models [1–16] have been proposed. However, due to unknown nature of the interface, inhomogeneity is not well understood.

The controlling mechanisms to the barrier height are not known yet sufficiently [17,18]. But, some theories exist in the literature [17–19] and these works are devoted to the relation of the barrier height distribution of Mo on p-GaTe.

In metal–semiconductor contacts, σ demonstrates the standard deviation of the barrier and it is the most important parameter that reflects directly greatness and effect of inhomogeneities and the interaction of the semiconductor with the metal. σ also presents a knowledge about distribution of the barrier that has single or multi Gaussian distribution. The existence of single or multi Gaussian distribution of barrier is to be related to semiconductor surface and/or interaction between deposited metal and semiconductor [18,19].

Barrier anomalies may cause different barrier height distributions. In each temperature, apparent effective barrier controls the main part of current across the junction. Thus may be a separate barrier distribution for each one temperature and each distribution may represented with a mean barrier height ϕ_b and its standard deviation σ. If one σ assumes as a parameter that is independent from temperature, then σ will have a mean value for each Gaussian distribution region that has been considered until now [12,16,20–23].

Thermionic emission theory [24,25] can depict ideal barrier structures and is based on the assumption of homogeneous Schottky barrier. However, inhomogeneities as observed from *I–V–T* curves are characterized with two different models. These are 'parallel conduction' [26] and 'pinch-off' models [13,14]. The parallel conduction model is used more due to its simplicity. The single [12] or multi-Gaussian [16] distribution model is based on the parallel conduction model that can depict barrier anomalies successfully. The single-Gaussian distribution model is insufficient to explain inhomogeneity in case of a multi barrier distribution [16,23]. A model to comment on discrete multi Gaussian distributions was proposed by Yu-Long et al. [16] and much more generalized form on Richardson plot of the multi-Gaussian distribution has been developed by Gülnahar and Efeoğlu [23].

In the literature, Richardson plots are drawn for Schottky structures having double or multi-Gaussian distributions and are analyzed separately for each distribution. In consequence Richardson constants are reported to have been a separate value for each distribution [9,12,22,39,46]. However, if effective mass is not changed with temperature, the Richardson constant should have a single value for all barrier distributions. Therefore, the modified Richardson plot should reorganize [22,39,46].

GaTe is a relatively known semiconductor compound [21–23,27–41,45,47] and exist successful but limited Schot-

* Corresponding author at: Erzincan University, Technical High School, Department of Electrics, 24200 Erzincan, Turkey.
E-mail address: mgulnahar@erzincan.edu.tr (M. Gülnahar).

0925-8388/$ – see front matter.
doi:10.1016/j.jallcom.2011.03.170

tky contact studies [21–23,37–40] made using GaTe. GaTe belongs to the III–VI group in the periodic table and has a layered nature. GaTe also has a monoclinic crystal structure and consists of successive Te–Ga–Ga–Te atomic planes joined together with Ga–Ga bonds lying approximately at right angles to other Ga–Ga bonds [27]. It has covalent bonds inside the layers and van der Waals type bonding between the layers [41].

The most reliable *I–V–T* properties of Schottky structure on p-GaTe have been reported by our early studies such as Al/p-GaTe [22] and Au/p-GaTe [23]. Double-Gaussian behavior of p-GaTe has been discussed in these studies. The results for each metallization suggest that the observed Gaussian distribution should be mainly related to the substrate. Besides, the occurrence of stair like surface of p-GaTe was reported [23,47] that may be a responsible mechanism for the Gaussian distribution during peeling process in fabrication stage. In the example of CdTe [17], the ratio of Te to Cd is reported to have been important at the interface of the sample.

The layers within GaTe are bounded by van der Waals type bonds and are expected to have no dangling bond theoretically on the surface. Heating of GaTe over 200 °C during annealing process may result in Te loss. This problem in p-GaTe may be overcome by capping or annealing under Te base pressure. It should be noted that annealing effect on p-GaTe is well known [32]. However, Te loss from GaTe is not expected due to self capping and fresh surfaces obtained by removing a layer of GaTe from surface after ohmic contact process followed for Schottky metalization.

According to the best of our knowledge, we have fabricated Schottky contacts on p-GaTe using sputtering for the first time. We have carried out an extensive *I–V–T* analysis and double barrier distribution found even for Mo/p-GaTe. Besides, the behavior of modified Richardson plot for the double distribution was recommented in this study.

2. Experiment

The mirror-like and highly smooth surface for GaTe may be obtained after layer removal and in consequence of this process is expected that the barrier inhomogeneities and the surface states should eliminate.

The metallization with In for ohmic contact on the backside of the p-GaTe was made by thermal evaporation at 8×10^{-8} Torr base pressure [22]. Besides, In evaporated thin samples are bonded to In/Au/Si substrate [22] and sintered at 225 °C for 2.5 min under a nitrogen flow [37]. Schottky metallization was made by sputtering. Metallization of Mo at 2×10^{-3} Torr Ar base pressure on a freshly cleaved surface was formed through a shadow mask with 0.5 mm diameter holes. Before metallization, the chamber was pumped down to 1×10^{-7} Torr pressure and plasma was formed at 2×10^{-3} Torr Ar base pressure. During sputtering, the current and voltage values applied to Mo target were stabilized at 100 mA and 390 V, respectively.

I–V–T measurements of the diodes were made using a closed cycle He cryostat at a range of 50–300 K temperature. The temperature was stabilized in 50 mK with a LakeShore 330 temperature controller while the voltage to the sample was applied with 5 mV steps driven by a Keithley 2400, and in consequence the current was measured by a Keithley 6514 electrometer using an automated measurement system [42].

3. Results and discussion

3.1. Forward-bias $I–V_T$ characteristics

Fig. 1 shows $I–V_T$ curves of a Mo/p-GaTe/In Schottky diode fabricated using sputtering, which are measured between 0 and 1 V forward bias at a range of 50–300 K temperature. As seen in Fig. 1, thermal emission is evident for all the measurement temperatures and the rectification ratio is high between 0 and 0.4 V bias values. However, the current above 0.4 V is limited by series resistance.

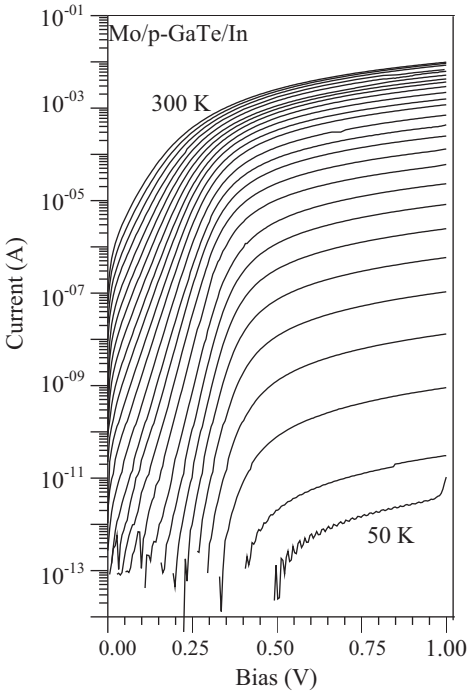

Fig. 1. Forward *I–V* characteristics of Mo/p-.

Cheng functions are used for *I–V* analysis of diodes which have high series resistance [43]. The series resistance values for our Mo/p-GaTe/In sample was calculated using Cheng functions expressed as,

$$\frac{dV}{d(\ln\ I)} = IR_s + n\left(\frac{kT}{q}\right) \tag{1}$$

$$H(I) = V - n\left(\frac{kT}{q}\right)\ln\left(\frac{I}{AA^*T^2}\right) \tag{2}$$

where $H(I)$ is given by

$$H(I) = IR_s + n\phi_b. \tag{3}$$

The series resistance values for Mo/p-GaTe/In using Eqs. (1–3) were obtained to be 55 Ω at 300 K and 54 MΩ at 80 K, which are lower than the series resistance values obtained for Al/p-GaTe/In [22] and Au/p-GaTe/In [23].

Series resistance of Schottky diodes with unintentially doped p-GaTe becomes effective especially at lower temperatures [22,23]. Thus, substrate may be related to series resistance, as clearly seen in Fig. 1. In a semiconductor, bulk resistance is dependent on temperature and is described by the following equation [25,44]

$$\frac{1}{R_s} \propto \sigma = C\ \exp\left(\frac{-E_a}{kT}\right) \tag{4}$$

where C is a constant. According to Eq. (4), the activation energy E_a can be calculated if $\ln(R_s)$ versus $1/T$ is linear. As seen in Fig. 2, there are two linear regions with two E_a activation energy, which are calculated to be 95.0 meV and 140.4 meV. Thus, there may be two deep acceptor levels located above the valance band of p-GaTe. A deep acceptor level located at 140 meV for p-GaTe has been reported in the electrical measurements [32].

Free carriers in unintentionally doped p-GaTe are supplied from deep acceptor levels [32]. Capacitance–voltage ($C–V$) [22] and thermally stimulated capacitance measurements ($C–T_V$) [45] made

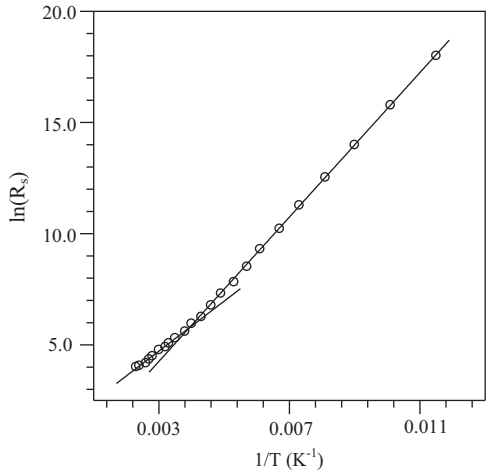

Fig. 2. Plot of $\ln(R_s)$ versus 1/T for a Mo/p-GaTe sample. The series resistance values of fabricated Schottky diode was calculated from Cheung functions for 80–300 K temperature range.

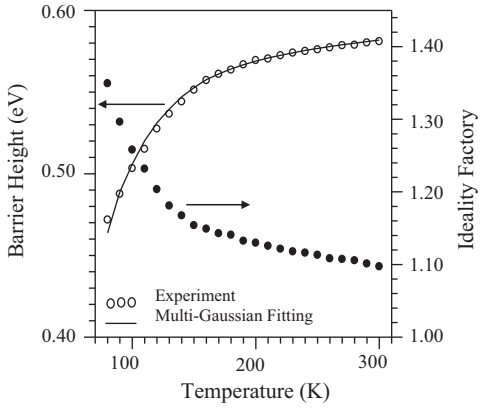

Fig. 3. The variations of the barrier height and ideality factor as a function of temperature. The continuous curve presents a multi-Gaussian curve after A_i arbitrary distribution function values in Table 1 and the fitting parameters as $\bar{\phi}_{bi}$ and σ_i between $i = 1$ and 23 dependent to the temperature obtained from Fig. 4 are substituted into Eq. (8).

on p-GaTe support these results. At lower temperatures, series resistance increases effectively which is expected as a result of freeze-out of the deep levels in p-GaTe. These observations indicate that semi-insulating behavior of unintentially doped p-GaTe is unavoidable below 80 K.

3.2. The barrier height and ideality factor characteristics of Mo/p-GaTe

In metal semiconductor contacts, the current transportation mechanism is explained with thermionic emission mechanism and non-ideal behaviors are based on thermionic emission equation [24,25]. The 'parallel conduction' model with the thermionic emission theory is successful in explanation of observed anomalies. According to 'parallel conduction' model, total current is considered as a sum of the currents flowing through all of the patches in which each Schottky barrier with different values makes contribution to total current [46]. The general *I–V* relationship with 'parallel conduction' model may be written as [26],

$$I = AA^*T^2 \left[\exp\left(\frac{qV}{nkT}\right) - 1\right] \int_0^\infty A(\phi_b) \exp\left(\frac{q\phi_b}{kT}\right) d\phi_b \quad (5)$$

where k is the Boltzmann constant, q is the electronic charge, A^* is the Richardson constant, T is the absolute temperature, V is the applied voltage, n is the ideality factor, ϕ_b is the barrier height, A is the diode area and $A(\phi_b)$ is an arbitrary Schottky barrier distribution function.

According to Thermionic emission theory, the ideality factor and the barrier height values from *I–V* curve can be calculated using well known equations in literature [9–25] as,

$$n = \frac{q}{kT}\frac{dV}{d(\ln I)} \quad (6)$$

$$\phi_b = -\frac{kT}{q} \ln\left(\frac{I_0}{AA^*T^2}\right) \quad (7)$$

where I_0 is the saturation current.

The barrier height and the ideality factor of the Mo/p-GaTe using Eqs. (6) and (7) from *I–V–T* curves of Fig. 1 was calculated to be 0.581 eV and 1.097 at 300 K and 0.472 eV and 1.349 at 80 K, respectively. Fig. 3 shows the variation of the ideality factor and barrier height with temperature, demonstrating strong dependence below 130 K.

In ideal metal–semiconductor contacts, ideality factor should be $n \approx 1$ for all temperatures and the barrier height should follow the variation of band gap with temperature. However, as seen in Fig. 3 a decrease in barrier height and an increase in ideality factor, especially below 130 K, is due to Schottky barrier inhomogeneities. Schottky barrier parameters are also influenced by free carrier density and ohmic contact behavior. However, ohmic contact in p-GaTe was optimized [37] and it is reported that freeze-out effect occurs below 130 K [23].

3.3. Temperature dependence of the barrier parameters

Spatial distribution of barrier anomalies is described by Gaussian distribution function which is used widely in the literature due to its simplicity and practical application to *I–V* measurements [12,16,21–23,39]. Gaussian distribution function can be applied easily, as seen in Fig. 4 in which distinct distributions are shown. Multi-Gaussian distribution approach is a model which obviously describes the distributions and can interpret inhomogeneities suc-

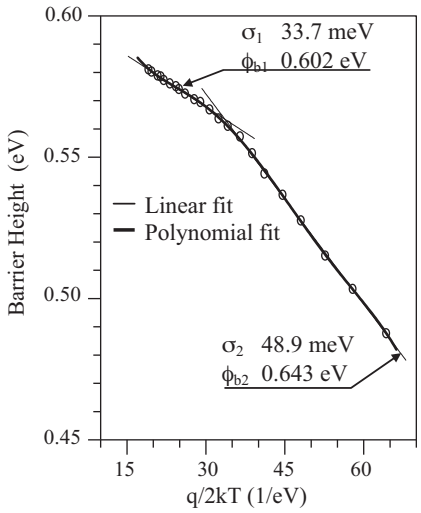

Fig. 4. Plot of the barrier height versus q/2*kT*. The discrete linear fits were carried out two barrier distributions. The continuous curve shows a polynomial fit made two distribution regions.

cessfully. According to this distribution model, the barrier height can be written as [16]

$$\phi_b = -\frac{kT}{q} \quad \ln \sum_{i=1}^{n} A_i \exp\left(-\frac{q\bar{\phi}_{bi}}{kT} + \frac{q^2\sigma_i^2}{2k^2T^2}\right) \tag{8}$$

In Eq. (8) A_i, σ_i and $\bar{\phi}_{bi}$ are the weight, standard deviation and mean barrier height of each Gaussian distribution, respectively. In condition that single Gaussian distribution model, the barrier height for $n = 1$ in Eq. (8) may be simplified to [12],

$$\phi_b = \bar{\phi}_{b1} - \frac{q\sigma_1^2}{2kT}. \tag{9}$$

σ_i and $\bar{\phi}_{bi}$ values are obtained by linear fittings to the distribution regions that demonstrate distinct linear variations of barrier height according to Eq. (9). So far, this approach has been used frequently in the literature [12,16,21–23,39] to obtain distribution parameters. According to this consideration, each distribution region is characterized by single mean σ_i and mean $\bar{\phi}_{bi}$. However, this approach is not applicable every time.

In metal–semiconductor contacts, the effect of barrier inhomogeneities is to cause variation in the values of ideality factor and barrier height with temperature. According to parallel conduction model, total current is the sum of the different currents flowing through various patches present. However, the barrier anomalies possibly influence the total current differently at each temperature. This means, the current flowing through each patch also varies with temperature. Therefore, a separate barrier height distribution exists at each temperature with respective values of mean barrier height, standard deviation and weight coefficient.

In Schottky barrier, n ideality factor reflects directly the effect of barrier anomalies and has a different value at each temperature. The relationship between the ideality factor and barrier height is expressed as [1],

$$\left(1 - \frac{1}{n}\right) = -\frac{d\phi_b}{dV} \tag{10}$$

If we reorganize Eqs. (9) and (10), relationship between standard deviation and ideality factor becomes clear. Thus, it may be expressed that σ_i demonstrates directly the effect of inhomogeneities with a big similarity to the behavior of n ideality factor. In addition, σ_i is related to the barrier height according to Eq. (9) and is seen that barrier height demonstrates dependence to temperature in the experimental studies [7–16,20–25]. In consequence, σ_i should be expressed as a function of the temperature and may not have a constant mean value for a distribution. Therefore, it is noted that the barrier should have a different distribution at each temperature and finally Eqs. (8) and (9) can be reorganized as a function of the temperature for each T_i. Furthermore, σ_i is not independent from a mean value of each distribution region. The difference between σ_i values at each distribution region should be small or big and close to each other, at nearness of a mean σ_i value of distribution obtained using classical method.

According to classical consideration [12,16,22,23,39] in which σ_i and $\bar{\phi}_{bi}$ parameters are independent from the temperature, those parameters are calculated using Eq. (9) from ϕ_b versus q/2kT plot. Fig. 4 shows the variation of ϕ_b with q/2kT for Mo/p-GaTe Schottky contact. In Fig. 4, two different linear regions appear according to classical Gaussian approach. In our previous works, these distributions have been seen for Al/p-GaTe [22] and Au/p-GaTe [23]. We reported that Schottky barrier of Al and Au on p-GaTe showed double-Gaussian behavior [22,23]. In Fig. 4, the standard deviation and mean barrier height values using Eq. (9) with linear fits to distribution regions for Mo/p-GaTe were calculated to be σ_i: 33.7 meV and 48.9 meV and $\bar{\phi}_{bi}$: 0.602 eV and 0.643 eV.

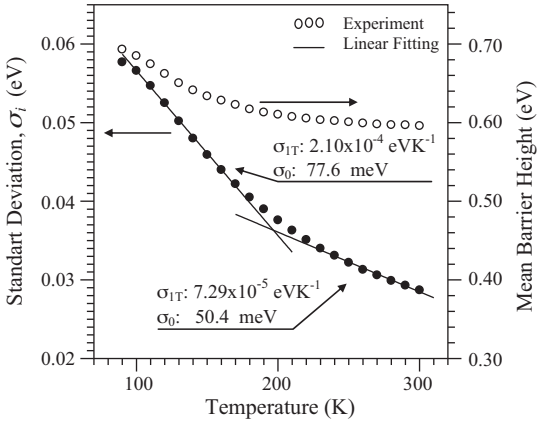

Fig. 5. Temperature dependence of the standard deviation (σ_i) and mean barrier height ($\bar{\phi}_{bi}$) obtained from Fig. 4 and discrete linear fits.

Standard deviation (σ_i) and mean barrier height ($\bar{\phi}_{bi}$) values for each temperature can be obtained by carrying out a polynomial fit of ϕ_b versus q/2kT data using Eq. (9). σ_i values can be found from the first derivative of best fit and mean barrier height ($\bar{\phi}_{bi}$) values then deduced from Eq. (9) itself. Fig. 4 presents a polynomial fit made along all barrier distributions. σ_i and $\bar{\phi}_{bi}$ parameters for Mo/p-GaTe were calculated to be 58.4 meV, 0.693 eV at 80 K and 29.7 meV, 0.596 eV at 300 K, respectively. Fig. 5 demonstrates σ_i and $\bar{\phi}_{bi}$ values for each measured temperature obtained according to this mentioned method. In Fig. 5, σ_i values represent two distinct linear variations with a big similarity to the variation of ϕ_b versus q/2kT in Fig. 4 and $\bar{\phi}_{bi}$ values vary more resolute with the temperature. Besides, σ_i have low values with a slope of 7.29×10^{-5} eV K^{-1} for all high temperatures and it varies reversely with a slope of 2.10×10^{-4} eV K^{-1} for low temperatures. This behavior of σ_i demonstrates clearly the effectiveness in different distribution regions of barrier inhomogeneities. In Fig. 5, the slope of σ_i may be expressed as the variation coefficient dependent on the temperature of the standard deviation and was given by σ_{iT}. In addition, σ_0 is the value of σ_i at $T = 0$ and is σ_{10}: 50.4 meV and σ_{20}: 77.6 meV, as seen in Fig. 5.

If one compares σ_i values in Fig. 5 with the mean σ_i values in Fig. 4 for two linear barrier distribution regions, it is seen that σ_i is 33.7 ± 4 meV for high temperatures and is 48.9 ± 9.5 meV for low temperatures. Thus, it is reported that σ_i values are obtained for each distribution region using a polynomial fit and vary at nearness of a mean σ_i value of the same distribution region.

Schottky barrier inhomogeneities are summed over infinite number of Gaussian distributions with different mean barrier heights and standard deviations. Therefore, using an arbitrary distribution function is more meaningful to depict inhomogeneities. This distribution function may be written as [16],

$$A(\phi_b) = \sum_{i=1}^{n} \frac{A_i}{\sigma_i\sqrt{2\pi}} \exp\left[-\frac{(\phi_b - \bar{\phi}_{bi})^2}{2\sigma_i^2}\right] \tag{11}$$

where A_i, σ_i and $\bar{\phi}_{bi}$ are the weight, the standard deviation and the mean barrier height of each Gaussian distribution, respectively.

According to multi-Gaussian distribution of the barrier, total of the A_i arbitrary distribution parameters under the normalization condition may be written as,

$$A_1 + A_2 + \ldots\ldots + A_n = 1 \tag{12}$$

and the total distribution function is expressed as,

$$A(\phi_b) = A_1(\phi_b) + A_2(\phi_b) + \ldots\ldots + A_n(\phi_b) \tag{13}$$

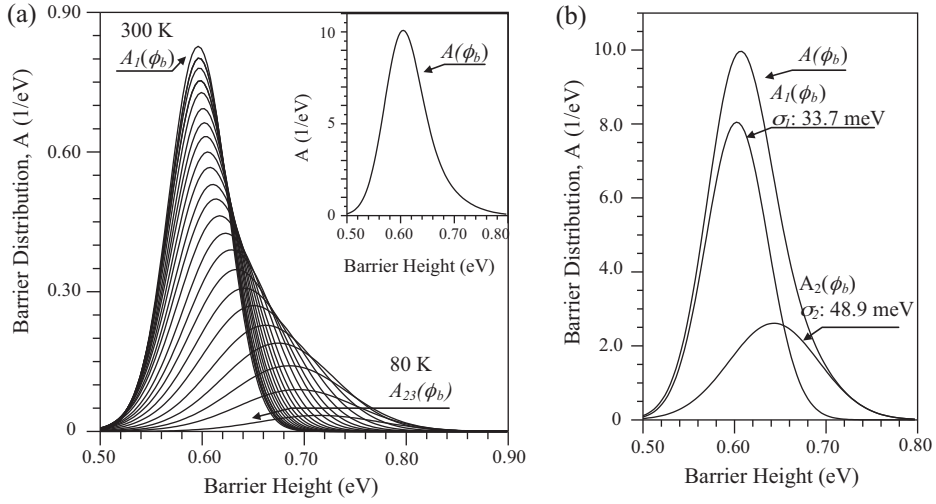

Fig. 6. (a) Distribution curves of the multi-Gaussian distribution function with σ_i and Φ_{bi} fitting parameters obtained from Fig. 4 for 80–300 K temperature range and the total Gaussian distribution function is shown in the inset. (b) Distribution curves of the double-Gaussian distribution function. The fitting parameter σ_1 are given in the figure and A_1: 0.69 and A_2: 0.31 are the weighting constants for each distribution.

Table 1
A_i arbitrary distribution parameter values iterated from Fig. 3 for a Mo/p-GaTe.

T (K)	Ai	T (K)	Ai
300	0.0595	180	0.047
290	0.0589	170	0.045
280	0.0585	160	0.043
270	0.0578	150	0.040
260	0.0571	140	0.037
250	0.056	130	0.034
240	0.055	120	0.030
230	0.054	110	0.026
220	0.0528	100	0.020
210	0.0516	90	0.013
200	0.0500	80	0.005
190	0.0488		

A_i arbitrary distribution parameters may be obtained by iteration. In Fig. 3, solid line on experimental data depicts Gaussian distribution values of the barrier height obtained with using in Eq. (8) of the fitting parameters from Fig. 4 for $n = 23$. According to multi-Gaussian distribution behavior, single curve on all experimental barrier height shown in Fig. 3 does not express that the barrier has only one Gaussian distribution. It includes to the contribution of all distribution regions of the barrier height. Consequently, is seen in Fig. 3 that Gaussian distribution is in good agreement with the experimental data. Besides, the A_i arbitrary distribution parameters for Mo/p-GaTe were also iterated between $n = 1$ and 23 at 80–300 K temperature range. The A_i values were obtained to be 0.005 at 80 K and 0.0595 at 300 K and these values for each temperature are shown in Table 1. In Table 1, the A_i values decrease with decreased temperature. This decrease is much more apparent below 130 K.

Mo/p-GaTe has a double barrier distribution according to the classical approach. A_1 and A_2 were obtained to be 0.69 and 0.31 by iteration, as shown with the solid line in Fig. 3. A_1: 0.69 and A_2: 0.31 values are nearly equal to $\sum_{i=1}^{n=12} A_i$ and $\sum_{i=13}^{n=23} A_i$ in Table 1, respectively. This demonstrates the agreement of the two models and the validity of this new approach.

Fig. 6(a) demonstrates $A_i(\phi_b)$ curves for each temperature between $n = 1$ and 23. $A_i(\phi_b)$ arbitrary distribution functions and $A(\phi_b)$ total distribution function were obtained using Eqs. (11)–(13). As shown in Fig. 6(b), the contribution of the $A_1(\phi_b)$ distribution at high temperatures is far greater than that of $A_2(\phi_b)$. This shows that dominant patches along Schottky area at high temperatures have 0.60 eV with a mean barrier height of 69% and have 0.64 eV with second mean barrier of 31% at low temperatures. Therefore, we can indicate that the contribution of the mean barrier observed at high temperatures is far greater than the contribution of the second mean barrier.

3.4. Richardson plot with multi-Gaussian distribution

From the thermoionic emission equation, the saturation current at $V = 0$ can be written as,

$$I_0 = AA^*T^2 \exp\left(-\frac{q\phi_b}{kT}\right) \tag{14}$$

By reorganizing Eq. (14), this equation may be rewritten as,

$$\ln\left(\frac{J_0}{T^2}\right) = \ln A^* - \frac{q\bar{\phi}_{bi}}{kT} \tag{15}$$

where $\bar{\phi}_{bi}$ is the mean zero voltage barrier height (or activation energy).

The variation of $\ln(J_0/T^2)$ as a function of $1/T$ is the Richardson curve, which is shown in Fig. 7 for Mo/p-GaTe. As seen in Fig. 7, the variation of $\ln(J_0/T^2)$ versus $1/T$ is linear for a wide temperature range. However, Schottky barrier anomalies are more active in the barrier especially below 130 K for Mo/p-GaTe and cause deviation from the linearity of the Richardson curve. In addition, these inhomogeneities occasion to calculating as a smaller value from A^* theoretical value of p-GaTe (for p-GaTe $A^* = 119.4\,\mathrm{AK^{-2}\,cm^{-2}}$ [38]) and $\bar{\phi}_{bi}$ mean barrier height value obtained from Fig. 4. A^* and $\bar{\phi}_{bi}$ values for Mo/p-GaTe were calculated to be $4.30\,\mathrm{AK^{-2}\,cm^{-2}}$ and 0.53 eV from the Richardson plot, respectively.

Non-ideal behaviors observed in the Richardson plots are due to non-homogeneous barrier distributions. To interpret this anomaly, Gaussian distribution function has been used frequently [21–23,39]. Eq. (15) is used to define only one single-Gaussian distribution on the Richardson plot and is meaningless for multi-Gaussian distribution. In the case of multi-Gaussian distribution, the Richardson equation can be reorganized to depict these anomalies successfully [23]. Therefore, Eq. (15) can be rewritten as [23],

$$\ln\left(\frac{J_0}{T^2}\right) = \ln A^* + \ln\sum_{i=1}^{n} A_i \exp\left(-\frac{q\bar{\phi}_{bi}}{kT} + \frac{q^2\sigma_i^2}{2k^2T^2}\right) \tag{16}$$

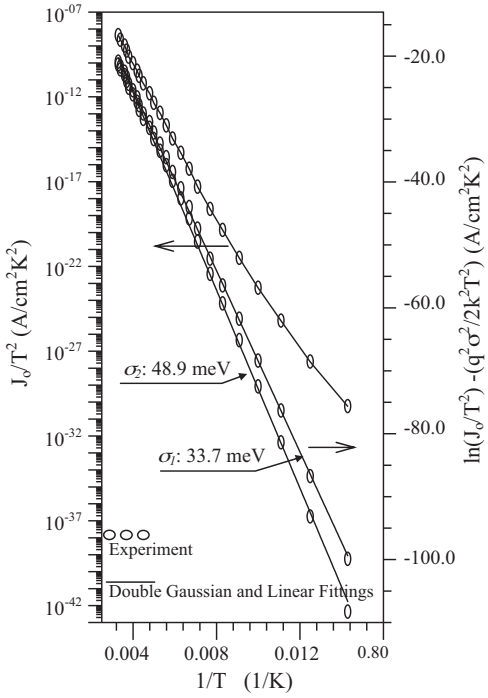

Fig. 7. The Richardson plot ($\ln(J_0/T_2)$ vs. $1/T$ variation) and the Modified Richardson plot of Mo/p-Gate ($\ln(J_0/T^2)$-$q^2\sigma^2/2k^2T^2$) vs. $1/T$ variation) and discrete linear fits. (The continuous curve in the Richardson plot shows double Gaussian obtained accroding to Eq. (16) by A^* Richardson constant value $A^* = 117.19\,\mathrm{AK^{-2}\,cm^{-2}}$ from Fig. 8, Φ_{bi} and σ_i from Fig. 4, A_i from Fig. 3).

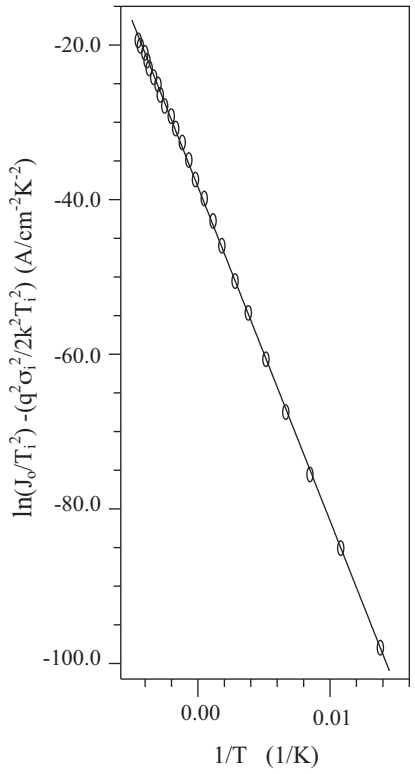

Fig. 8. The modified Richardson plot of Mo/-Gate ($\ln(J_0/T_i^2) - (q2\sigma_i^2/2k^2/T_i^2)$ vs. $1/T$ variation) with σ_i values presented in Table 1 and its discrete linear fits.

Under single-Gaussian distribution condition, Eq. (16) for each barrier distribution and T_i temperature may be expressed as,

$$\ln\left(\frac{J_{0i}}{T_i^2}\right) = \ln A^* - \frac{q\bar{\phi}_{bi}}{kT_i} + \left(\frac{q^2\sigma_i^2}{2k^2T_i^2}\right) \tag{17}$$

Eq. (17) is a modified Richardson equation having a single-Gaussian distribution [12,21,22,39]. A^* is a constant in Eq. (17), where effective mass is defined by energy band diagram of semiconductor and is expected to be independent from temperature.

According to the classical model, Mo/p-GaTe has double-Gaussian distribution with σ_1: 33.7 meV and σ_2: 48.9 meV mean standard deviations. A^* Richardson constant values calculated using Eq. (17) from the modified Richardson plot in Fig. 7 have two different values one of which is $102.88\,\mathrm{AK^{-2}\,cm^{-2}}$ for σ_1: 33.7 meV and the other is $129.19\,\mathrm{AK^{-2}\,cm^{-2}}$ for σ_2: 48.9 meV. These A^* values are far from the theoretical A^* value given in the literature [38]. Thus, the modified Richardson plot is unsuccessful if one considers independently each distribution, as shown in Fig. 7.

The failure of the modified Richardson plot can be overcome with our new approach in which the barrier has got a separate barrier distribution for each temperature. The linearization at only single line of the modified Richardson plot for multi-barrier distributions may be obtained by subtraction to $(q^2\sigma_i^2/2k^2T_i^2)$ values from experimental $\ln(J_{oi}/T_i^2)$ values using σ_i values obtained from Fig. 4 for each T_i temperature. Fig. 8 shows the new modified Richardson plot according to our approach, which is different from Fig. 7 and has only one straight line for the temperature range used in experiment. According to Eq. (17), the Richardson constant A^* from Fig. 8 was calculated to be $117.19\,\mathrm{AK^{-2}\,cm^{-2}}$ and is close to the theoretical value of p-GaTe [38].

4. Conclusions

In metal–semiconductor contacts, Schottky barrier inhomogeneities are responsible mechanisms for anomaly behaviors observed in barrier height, ideality factor and Richardson plots when measurement temperature was reduced. Gaussian distribution model to depict these anomalies is used frequently and is rarely successful, as reported in the literature [12,20–22,39]. To overcome these difficulties, we have presented a model on the basis of a multi-Gaussian distribution model.

A molybdenum Schottky contact on p-GaTe was fabricated under optimum conditions using sputtering method. *I–V–T* properties of Mo/p-GaTe were interpreted using the thermionic emission theory and the Gaussian distribution was observed to be double as reported in the literature [22,23].

Multi-Gaussian distribution function to explain the anomalies can be depicted successfully with a mean standard deviation and a mean barrier height for each distribution region. However, in this work was discussed a different approach. Here, we considered distinct barrier distributions which control the main component of current across the barrier for each temperature. In consequence, it was noted that the barrier parameters ($\bar{\phi}_{bi}$ and σ_i) should represent a distribution for each temperature value. Besides, we discussed that $\bar{\phi}_{bi}$ and σ_i pairs independent from the temperature are not adequate for the calculation of the true Richardson constant. Therefore, $\bar{\phi}_{bi}$ and σ_i should change as a function of the temperature at nearness of their mean values. As a result, the anomalies on the basis of a multi-Gaussian distribution function were depicted successfully as a function of the temperature.

The Richardson constant should have a single value at all conditions. Thus, this problem in the modified Richardson plot was overcome using our new approach and the plot was drawn again. In consequence, the Richardson constant value for Mo/p-GaTe was calculated to be $117.19\,\mathrm{AK^{-2}\,cm^{-2}}$ from the new modified

Richardson plot and this value is very close to the theoretical Richardson constant of p-GaTe [38].

Acknowledgment

This work was supported by TUBITAK (The Scientific and Technological Research Council of Turkey) under the grant of 105T104.

References

[1] C.R. Crowell, S.M. Sze, Solid State Electron. 9 (1966) 1035–1048.
[2] F.A. Padovani, R. Stratton, Solid State Electron. 9 (1966) 695–707.
[3] W. Tantraporn, J. Appl. Phys. 41 (11) (1970) 4669–4671.
[4] V.L. Rideout, C. Crowell, Solid State Electron. 13 (1970) 993–1009.
[5] H.C. Card, E. Rhoderick, J. Phys. D: Appl. Phys. 4 (1971) 1589–1601.
[6] H.C. Card, E. Rhoderick, J. Phys. D: Appl. Phys. 4 (1971) 1602–1611.
[7] Y.P. Song, R.L. Van Meirhaeghe, W.H. Laflere, F. Cardon, Solid State Electron. 29 (6) (1986) 633–638.
[8] Maeda Keiji, Umeza Ikuro, Ikoma Hideaki, Yoshimura, Takahiro, J. Appl. Phys. 68 (6) (1990) 2858–2867.
[9] W.L. Chin Vıncent, M.A. Green, W.V. Storey John, Solid State Electron. 33 (2) (1990) 299–308.
[10] M.P. Hernandez, C.F. Alonso, J.L. Pena, J. Phys. D: Appl. Phys. 34 (2001) 1157–1161.
[11] H. Güttler Herbert, H. Werner Jürgen, Appl. Phys. Lett. 56 (12) (1990) 1113–1115.
[12] J.H. Werner, H.H. Güttler, J. Appl. Phys. 69 (3) (1991) 1522–1533.
[13] R.T. Tung, Phys. Rev. B 45 (23) (1992) 13,509–13,522.
[14] J.P. Sullivan, R.T. Tung, M.R. Pinto, W.R. Graham, J. Appl. Phys. 70 (12) (1991) 7403–7424.
[15] J. Osvald, Solid State Electron. 35 (11) (1992) 1629–1632.
[16] J. Yu-Long, R. Guo-Ping, L. Fang, Q. Xin-Ping, L. Bing-Zong, L. Wei, L. Ai-Zhen, Chin. Phys. Lett. 19 (2002) 553–556.
[17] R.L. Van Meirhaeghe, R. Van de Walle, W.H. Laflere, F. Cardon, J. Appl. Phys. 70 (4) (1991) 2200–2203.
[18] I.M. Dharmadasa, J.M. Thornton, R.H. Williams, Appl. Phys. Lett. 54 (2) (1989) 137–139.
[19] W. Mönch, Appl. Phys. Lett. 72 (15) (1998) 1899–1901.
[20] Chand Subbash, Kumar, Jitendra, Semicond. Sci. Technol. 11 (1996) 1203–1208.
[21] Coşkun Cevdet, Biber Mehmet, Efeoğlu, Hasan, Appl. Surf. Sci. 211 (2003) 360–366.
[22] M. Gülnahar, H. Efeoğlu, Balkan Phys. Lett., Special Issue (2008) 542–550.
[23] M. Gülnahar, H. Efeoğlu, Solid State Electron. 53 (2009) 972–978.
[24] E.H. Rhoderick, R.H. Williams, Metal-Semiconductor Contacts, 2nd ed., Oxford, Clarendon, 1988.
[25] S.M. Sze, Physics of Semiconductor Devices Second Edition, John Wiley and Sons, New York, 1981.
[26] I. Ohdomari, K.N. Tu, J. Appl. Phys. 51 (7) (1980) 3735–3739.
[27] W.B. Pearson, Acta Cryst. 17 (1964) 1–15.
[28] J.G. Antonopoulos, T.H. Karakostas, G.L. Bleris, N. Economou, J. Mater. Sci. 16 (1981) 733–738.
[29] Balitskii O.A., Jaegermann W. Mater. Chem. Phys., 97, 98–101.
[30] Güder H. S., Abay B., Efeoğlu H., Yoğurtçu Y. K. J. Luminescence, 93, 243–248.
[31] Taylor R.A, J.F. Ryan, J. Phys. C: Solid State Phys. 20 (1987) 6175–6187.
[32] H. Efeoğlu, T. Karacali, B. Abay, Y.K. Yoğurtçu, Semicond. Sci. Technol. 19 (2004) 523–530.
[33] Gülnahar M. Current–voltage and capacitance–voltage characteristics on temperature dependent of Al-Au/p-GaTe Schottky contact structures. Ph.D. Thesis. Atatürk University, Erzurum (Turkey): Unpublished (2000).
[34] Pal S., Bose D.N. Solid State Commun., 97(8), 725–729.
[35] L. Gouskov, A. Gouskov, Solid State Commun. 28 (1978) 99–105.
[36] C. Manfredotti, R. Murri, A. Rızzo, L. Vasanelli, G. Micocci, Phys. Stat. Sol. (a) 29 (1975) 475–480.
[37] C. Coskun, H. Efeoğlu, Semicond. Sci. Technol. 18 (2003) 23–27.
[38] G. Çankaya, B. Abay, Semicond. Sci. Technol. 21 (2006) 124–130.
[39] B. Abay, G. Çankaya, H.S. Güder, H. Efeoğlu, Y.K. Yoğurtçu, Semicond. Sci. Technol. 18 (2003) 75–81.
[40] D.N. Bose, S. Pal, Philos. Mag. B 75 (2) (1997) 311–318.
[41] J.Z. Wan, J.L. Brebner, R. Leonelli, G. Zhao, J.T. Graham, Phys. Rev. B 48 (1993) 5197–5201.
[42] Efeoğlu H. Automation program of Measure and Analyse for *I–V* and *C–V*. Unpublished (2005).
[43] S.K. Cheung, N.W. Cheung, Appl. Phys. Lett. 49 (2) (1986) 85–87.
[44] W.P. Kang, J.L. Davidson, Y. Gürbüz, D.V. Kerns, J. Appl. Phys. 78 (2) (1995) 1101–1107.
[45] Gülnahar M., Efeoğlu H. C–T_v measurements of Au/p-GaTe. Unpublished (2008).
[46] S. Zhu, R.L. Van Meirhaeghe, C. Detavernier, F. Cardon, G.P. Ru, X.P. Qu, B.Z. Li, Solid State Electron. 44 (2000) 663–671.
[47] O.A. Balitskii, B. Jaeckel, W. Jaegermann, Phys. Lett. A 372 (2008) 3303–3306.